

## Water Column Characteristics from Modern CTD Data, Lake Malawi, Africa

John D. Halfman

Department of Civil Engineering and Geological Sciences  
University of Notre Dame  
Notre Dame, Indiana 46556-0767

**ABSTRACT.** Conductivity, temperature, and dissolved oxygen profiles from Lake Malawi (Lake Nyasa), East Africa, provide a modern snapshot of water column characteristics during January, 1992. Temperature and dissolved oxygen concentration of the water column generally decrease with depth from over 28°C and over 80% saturation at the surface to just below 22.7°C and anoxic conditions deeper than 300 m. Specific conductance ( $\kappa_{25}$ ) of the water column typically increases with depth from 258  $\mu\text{S cm}^{-1}$  at the surface to 270  $\mu\text{S cm}^{-1}$  at 690 m with approximately 50% of the increase between 160 and 240 m. The increase in salinity complements a decrease in temperature across the chemocline to restrict vertical mixing during the rainy, warm season, and salinity may be the only barrier to vertical mixing across the chemocline during the windy, cool season. However, fluctuating bottom-water temperatures, compiled over the past 50 years from the deep-basin of the lake, suggest that cooler surface or near surface water is occasionally introduced into the monimolimnion. Conductivity profiles offshore of the Ruhuhu River show a mid-depth (30 - 65 m) layer of relatively fresh water (minimum of 213  $\mu\text{S cm}^{-1}$ ) that is interpreted as an interflow injection of river discharge. The discharge introduces surface or near surface waters to deeper depths in the lake.

**INDEX WORDS:** Lake Malawi, CTD data, water column mixing, tropical rift lakes.

### INTRODUCTION

The importance of large lacustrine basins for hydrocarbon accumulations, mineral deposits, and paleoclimatic studies has become more apparent in recent years. The tropical rift lakes of East Africa are excellent modern-day laboratories to understand these processes. Fundamental to these processes is the physical limnology. Our understanding of the physical limnology of Lake Malawi is based on only a few measurements taken during the 1970s and earlier. Since then, the detection of various physical properties has greatly improved through the development of new electronic instrumentation. This paper presents temperature, conductivity, and dissolved oxygen data measured by an internally recording CTD in Lake Malawi during January, 1992. The goal is to compare these data with earlier work and discuss the implications on the physical limnology of the basin.

Lake Malawi (Lake Nyasa), the fifth largest lake in the world, is located at the southern end of the East African Rift system (Fig. 1). It is approxi-

mately 570 km long by 75 km wide and has mean and maximum depths of about 270 and 700 m, respectively. Seasonal variations in precipitation, wind, and air temperature define the annual climatic cycle. The hydrologic budget is primarily controlled by precipitation, river runoff, and evaporation (Pike 1964, Beadle 1981). Input to the lake is skewed to the western shore due to pre-rift drainage patterns and, to a lesser extent, to the north from a gradient in rainfall (Beadle 1981, Crossley 1984). The Shire River, at the southern end of the lake, presently removes 20% of the total water loss but has been closed during historic and earlier episodes (Beadle 1981, Scholz and Rosendahl 1988, Owen *et al.* 1990, Finney and Johnson 1991).

Eccles (1962, 1974) and others (Beauchamp 1953, Jackson *et al.* 1963, Ferro 1977) have suggested that Lake Malawi is meromictic, i.e., similar to Lake Tanganyika. Temperatures within the mixolimnion experience distinct seasonal variability. Surface temperatures vary from just below 23°C



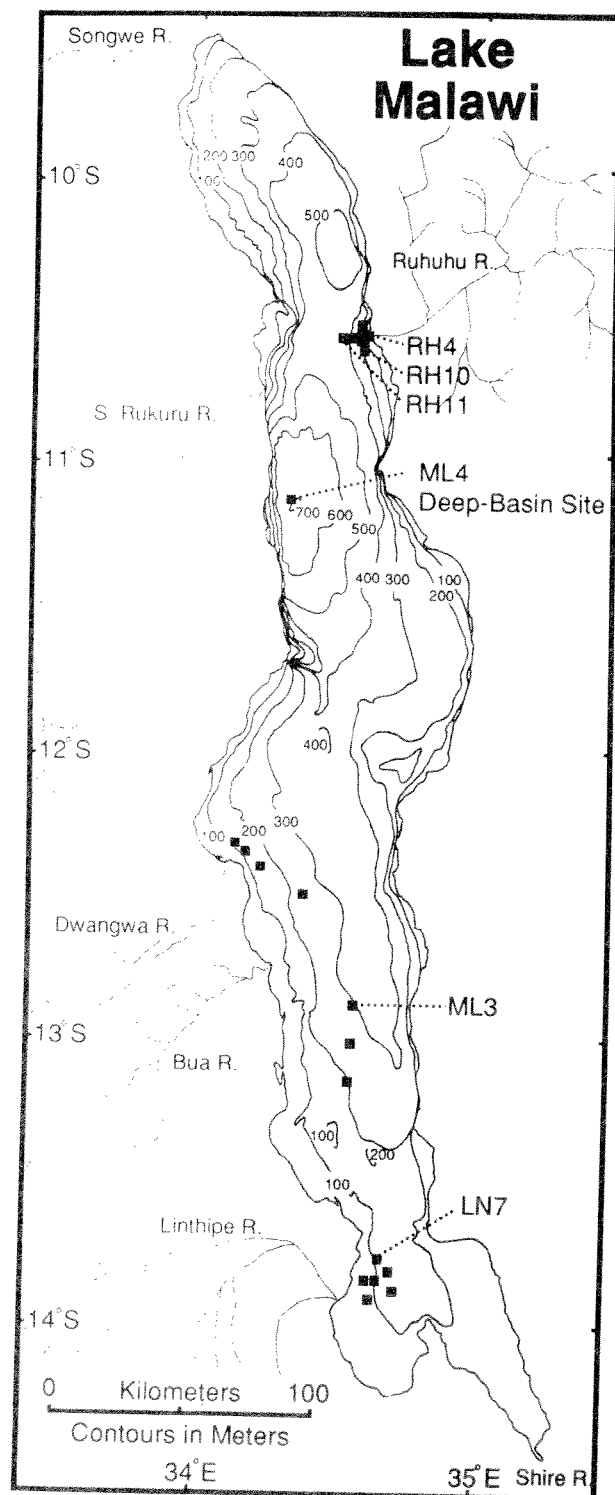


FIG. 1. Bathymetric map of Lake Malawi (modified from Johnson et al. 1988). Contours are in meters. CTD stations are plotted on the map (■) and identified if mentioned in the text. Nearshore stations, with water depths less than 5 m, are not plotted for clarity but are shown in Halfman and Scholz (1993).

in July and August (austral winter) to above 28°C in late February to early March (austral summer). A thermocline (within the mixolimnion) develops during the warm season as deep as 100 m. Two processes are postulated to maintain the mixolimnion to depths of 200 to 250 m: (1) Surface water cooling is especially strong in the lake's southeastern arm during austral winter, and gives rise to 21°C profile-bound currents that flow northward along the lake floor and presumably replace the lower mixolimnion waters further north. (2) Strong southerly winds (>25 knots) called Mweras mix the upper portions of the water column during the windy season (May to October) in addition to generating surface currents and internal seiches.

Temperature is postulated to control stratification at the chemocline ( $\approx 250$  m; Eccles 1974, Beadle 1981). Water temperatures are isothermal ( $22.7 \pm 0.03^\circ\text{C}$ ) but cooler below this depth than above. The monimolimnion is anoxic. The major dissolved ion concentrations at the deep basin site are (average and range of the data): calcium,  $0.96 \text{ meq L}^{-1}$  ( $0.88\text{--}1.01$ ); magnesium,  $0.63 \text{ meq L}^{-1}$  ( $0.61\text{--}0.63$ ); sodium,  $0.89 \text{ meq L}^{-1}$  ( $0.87\text{--}0.91$ ); and bicarbonate,  $2.43 \text{ meq L}^{-1}$  ( $2.31\text{--}2.51$ ) with smaller amounts of chloride, potassium, and sulfur species (Gonfiantini et al., 1979). Concentrations typically increase with depth, and parallel a rise in specific conductance detected at this station, from an average  $248 \mu\text{S cm}^{-1}$  ( $247\text{--}251$ ) in the upper 75 m of the water column to about  $265 \mu\text{S cm}^{-1}$  ( $264\text{--}268$ ) below 300 m.

## METHODS

Water column profiles of temperature and conductivity ( $\kappa_{25}$ ) were obtained electronically with an internally recording CTD (SEACAT SBE-19 with a narrow-range,  $0\text{--}0.6 \text{ S m}^{-1}$ , conductivity sensor). The instrument was interfaced with a polarographic oxygen sensor (SBE-23Y) and aspirating pump. Deployment rates were approximately  $1 \text{ m s}^{-1}$ , and data were downloaded to an IBM-compatible computer for storage and latter analysis. Data reproducibility for temperature was  $0.01^\circ\text{C}$ , specific conductance  $0.14 \mu\text{S cm}^{-1}$ , and dissolved oxygen  $0.17 \text{ mL L}^{-1}$ ; these estimates were computed by calculating the average difference of the respective values between the down-cast and up-cast data selected at 2-m increments after aligning the data with respect to time. A multiple cast to water depths just below 200 m at ML4, the deepest station, reveals down-cast data that are within to three times smaller than the stated reproducibilities above. The sensors were calibrated at the Northeast Regional Calibration Center before and after shipping the profiler overseas to test for drift. The new cali-

brations yield results that are within the reproducibilities stated above except for conductivity. Conductivities reported here utilize the earlier calibration and yield data that are, on average,  $1.2 \mu\text{S cm}^{-1}$  higher than those calculated by the new calibration. Conductivity to salinity conversions utilized the PSS-78 equations of Hill *et al.* (1986) and density calculations utilized the PVT equations of Chen and Millero (1977, 1986), where both equations stress freshwater (0–0.6 ‰) applications. No additional water samples were collected during this cruise. Thus, the accuracy but not the precision of the conversions should be regarded with caution because the chemical composition of dissolved ions in Lake Malawi is not proportional to that of seawater.

Twenty-eight stations were occupied during January, 1992 (Fig. 1). Station locations were primarily offshore the Linthipe (LN), Dwangwa (DW), and

Ruhuhu (RH) rivers to investigate the influence of fluvial inputs to the lake but also include four Mid-Lake (ML) sites that delineate a transect along the axis of the lake. The northern most Mid-Lake site (ML4) occupied a hydrograph station of earlier workers within the deepest basin of the lake. The remaining sites are restricted to water depths < 5 m and are clustered near the mouths of the Linthipe and Ruhuhu rivers. Locations were determined by global positioning satellite navigation with an accuracy greater than  $\pm 15$  m and on one occasion by radar when satellites were not available.

## RESULTS

The changes in temperature, dissolved oxygen, and conductivity with water depth are remarkably uniform throughout the lake (Figs. 2 & 3, Table 1).

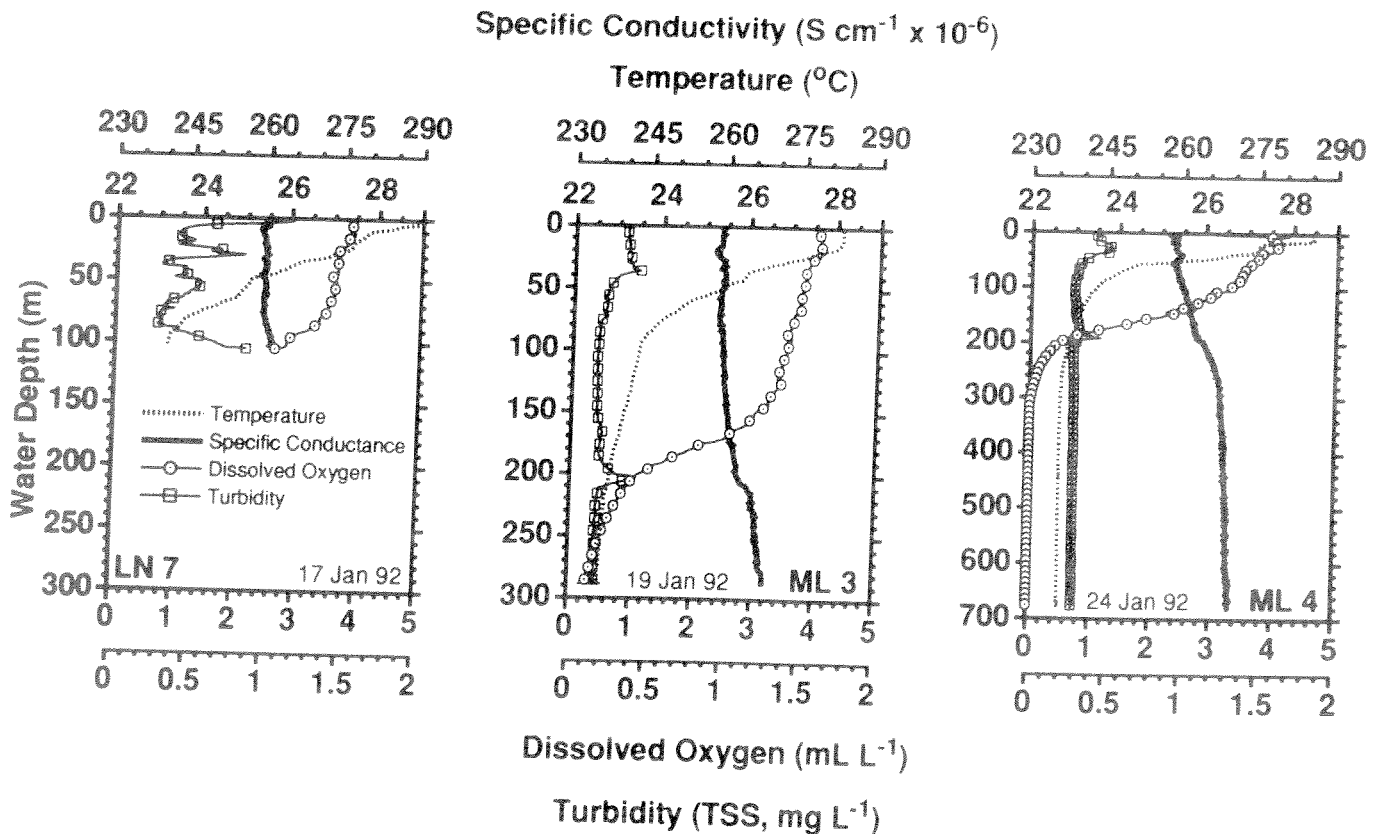


FIG. 2. Down-cast temperature (■), specific conductance (—,  $\kappa_{25}$ ) and dissolved oxygen (○) profiles for three stations in Lake Malawi along a north-south transect. Site ML4 reoccupied the deep-basin hydrograph station of earlier workers. These profiles are representative of the other stations on this cruise except for profiles offshore of the Ruhuhu River (Fig. 3). Turbidity profiles (□) are redrawn from Halfman and Scholz (1993). Note the change in depth scale for the deep basin profiles (ML4).

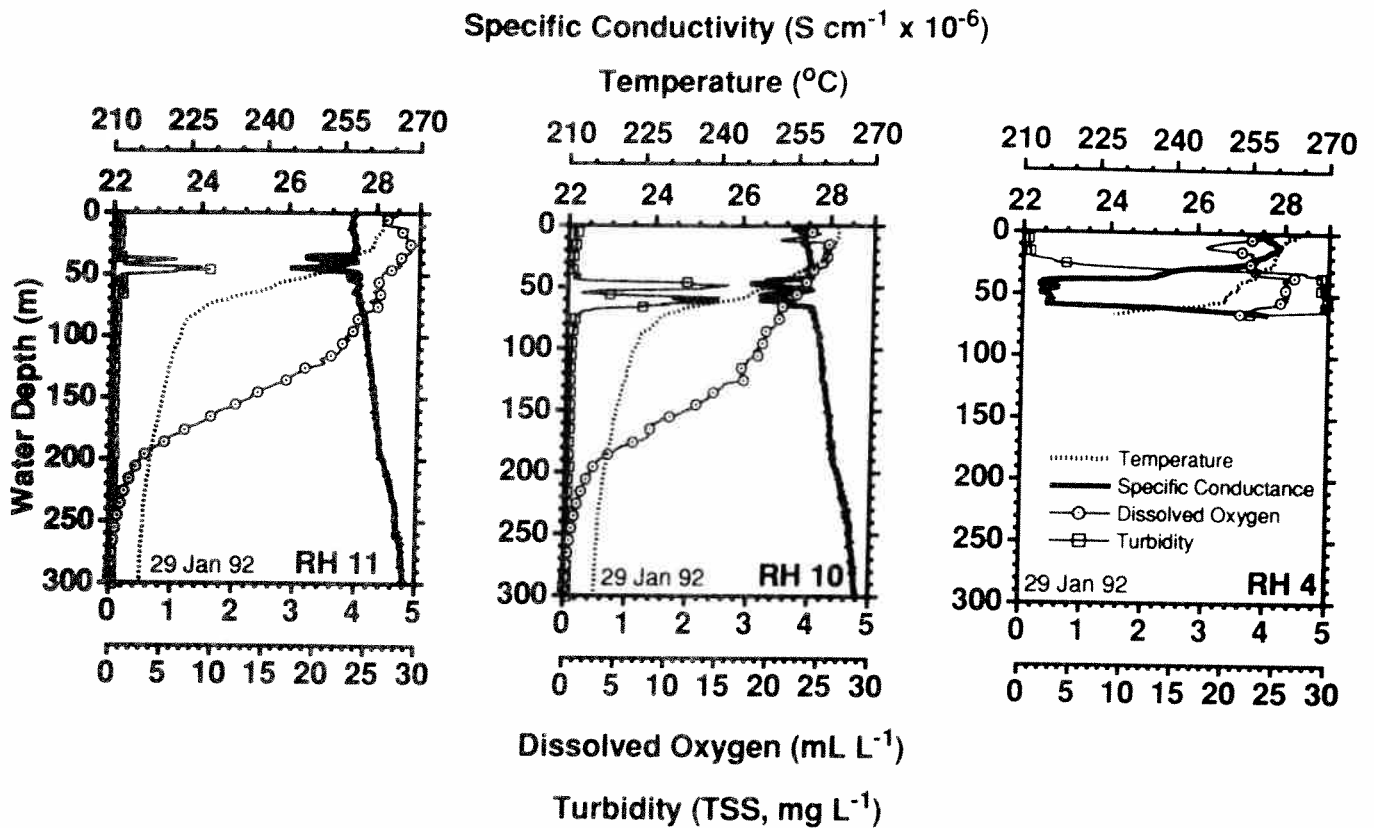


FIG. 3. Down-cast temperature (■ ■ ■ ■ ■), specific conductance (—,  $\kappa_{25}$ ) and dissolved oxygen (○) profiles from offshore of the Ruhuhu River. The stations are orientated along an east-west transect with increasing distance from the river mouth to the left. Turbidity (□) profiles are redrawn from Halfman and Scholz (1993). Note the change in scale for specific conductance and turbidity from Figure 2.

TABLE 1. Summary of specific conductance, temperature, and dissolved oxygen data.

Depth (m)		Conductance ( $\mu\text{S cm}^{-1}; 25^\circ\text{C}$ )	Temperature ( $^\circ\text{C}$ )	Dissolved Oxygen ( $\text{mL L}^{-1}$ )
0 to 80*	Mean	257.6	26.15	3.7
	Range	254.6-259.2**	23.73-28.51	3.4-4.0
80 to 200	Mean	261.2	23.21	2.3
	Range	259.2-263.9	22.87-23.72	0.7-3.4
200 to 300	Mean	266.5	22.75	0.2
	Range	264.0-267.7	22.69-22.87	0.0-0.7
300 to 700	Mean	269.0	22.68	0.0
	Range	267.6-270.1	22.67-22.70	0.0-0.0

\*Compilation excludes nearshore stations with water depths less than 5 m.  
 \*\*Individual profiles offshore the Ruhuhu River exceed this range.

For example, the standard deviation of each parameter at 0.75 m successive depth slices along the offshore profiles (sites with a water depth > 50 m) is usually less than the thickness of the line in the respective plot. Data from below 200 m reveal the greatest similarity, but this may be an artifact of only nine stations sampling depths greater than 200 m and two stations sampling depths below 350 m. Exceptions to the uniformity occur at water depths shallower than 100 m, especially offshore of the Ruhuhu River (Fig. 3).

Temperature generally decreases with water depth, from above 28°C to below 23°C (Figs. 2 & 3). The greatest variability from the typical profile is within the upper 80 m of the water column. For example, surface temperatures range from 27.95 to 29.30°C with the warmest temperatures detected at the southern-most stations on calm, sunny days. Individual temperature profiles typically reveal one or more sharp steps in the temperature gradient ( $dT/dz$ ) that are not at the same depth through out the lake but are above the main thermocline. The main thermocline at the Mid-Lake and Ruhuhu stations is deeper than at the other sites (between 50 and 70 m compared to 40 and 50 m, respectively) but none of the sites reveal a thermocline as deep as earlier reports. At depths below 80 m, temperature continues to decline to 22.66°C at 350 m but then warms to 22.70°C by 680 m.

Dissolved oxygen concentrations generally decrease with depth from above 4.0 mL L<sup>-1</sup> (above 80% saturation) to anoxic conditions (Figs. 2 & 3, Table 1). A maximum concentration of 4.9 mL L<sup>-1</sup> (27.8°C) was detected at 30 m below the surface at RH11. The transition to anoxic conditions is between 200 to 300 m based on up-cast and down-cast profiles, respectively.

Specific conductance ( $\kappa_s$ ) of the water column typically increases from 258  $\mu\text{S cm}^{-1}$  at the surface to slightly above 270  $\mu\text{S cm}^{-1}$  at the bottom of the lake (Figs. 2 & 3, Table 1). Fifty percent of the increase in conductivity with depth is between 160 and 240 m. The transition occurs significantly below the thermocline but brackets the upper limit of the chemocline as defined above.

Stations adjacent to the Ruhuhu River reveal atypical CTD profiles (Fig. 3.). Specific conductivity is lower than typical open-lake values, as low as 213  $\mu\text{S cm}^{-1}$  between depths of 30 and 65 m; whereas, values are more typical of open-lake conditions at shallower and deeper depths. This low conductivity layer is traceable from the mouth of the river (RH4) to sites almost 10 km to the west

and 5 km to the south. When present, the magnitude of the conductivity lowering and thickness of the layer decreases with increasing distance from the river mouth. The base of the low conductivity layer coincides with the thermocline. The dissolved oxygen profile at the site closest to the river mouth (RH4) reveals higher dissolved oxygen concentrations within the layer than typical values at open-lake sites. Above and below the layer at RH4 as well as the other stations offshore of the Ruhuhu, the dissolved oxygen profiles are similar to open-lake conditions.

### DISCUSSION

Temperatures profiles in the mixolimnion are similar to previous results for this season. Climatic variability (e.g., solar heating and wind stress) and geographic location can explain the differences in water temperatures above the thermocline. Deep-water temperatures at the deep-basin station (ML4) reveal a small rise in temperature of approximately 0.1°C between 350 and 700 m. The thermal inversion was not reported by earlier workers but the trend may have been hidden within the scatter of the earlier temperature data. The inversion can be accounted for by adiabatic temperature changes with water depth, i.e., calculated potential temperatures ( $T_p$ , adiabatically adjusted for pressure) cool by 0.04°C from 350 to 690 m. Geothermal heat from the earth's deep interior is postulated to warm the bottom waters in Lake Tanganyika (Coulter and Spigel 1991). It may warm the bottom waters in Lake Malawi, but it is not necessary to generate the observed profile.

Dissolved oxygen profiles within the upper 200 m of the lake are consistent with previous data. The decline with water depth is consistent with an input of dissolved oxygen by advection and diffusion at the lake surface, and net-photosynthesis in the euphotic zone balanced by the consumption of dissolved oxygen by net-respiration and chemical oxidation reactions. The up-cast and down-cast profiles position the chemocline, the transition to anoxic conditions, at 200 or 300 m, respectively. The range in water depths for the transition is commonly ascribed to slow response times of polarographic probes versus deployment rates, especially at low oxygen concentrations, and poisoning of the electrode by other gasses present in anoxic conditions. Unfortunately, we could not sample lake water deeper than 50 m. However, additional evidence positions the chemocline closer to 200 m. Approximately 50% of the increase in specific conductance occurs across the upper boundary (see

below). A turbid layer at or just above 200 m is interpreted as chemosynthetic bacteria or iron and manganese oxyhydroxides accumulating just above anoxic conditions (Halfman and Scholz 1993). Finally, the lowest depth with detectable dissolved oxygen in the earlier data sets is at or just below 200 m with only sporadic reports of detectable oxygen from depths below 250 m (Beadle 1981).

Specific conductance ( $\kappa_{25}$ ) increases with water depth. A similar increase in conductance was observed earlier (June, 1976) at the deep-basin station (Gonfiantini *et al.* 1979). The 1976 conductivity and lake chemistry data indicate that the conductance to salinity conversion underestimates ( $\approx 0.1 \text{ g kg}^{-1}$ ) the salinity predicted by the total mass of dissolved ions in 1 kg of lake water. The discrepancy may partially reflect different constants in the specific conductance to conductivity conversion (the earlier constants are unknown but may contribute to 20% of the offset) but probably reflects the dissimilarity of the dissolved ion chemistry between Lake Malawi and the ocean. However, the percent increase in water salinity between the surface ( $N = 5$  from 0 to 100 m) and bottom ( $N = 9$  from 300 to 700 m) of the lake that is predicted by the conductivity profiles is identical to that predicted by the distribution of the major dissolved ions with depth. The similarity suggests that the distribution of the major ions, that includes conservative species like chloride, controls the water conductivity to a greater extent than the distribution of charged biological nutrients or reduced ions. Historically, conductance values reported here are slightly larger ( $5$  to  $10 \mu\text{S cm}^{-1}$ ) and the surface to bottom-water range of values is slightly less ( $5 \mu\text{S cm}^{-1}$ ) than earlier measurements. Both changes are consistent with an actual increase in evaporation relative to precipitation within the basin over the past few decades but may instead be an artifact of different conversion constants mentioned above or the season of the profiles.

Previously, temperature was postulated as the control on vertical stability in the water column (Beadle 1981). The increase in dissolved ions across the chemocline may influence the density structure at this depth as well. The increase in specific conductance from  $260 \mu\text{S cm}^{-1}$  at 150 m ( $23.13^\circ\text{C}$ ) to  $266 \mu\text{S cm}^{-1}$  at 250 m ( $22.74^\circ\text{C}$ ) coupled with the decrease in temperature yields an increase in density ( $\Delta\rho_{s,t,0}$ ) of  $9.4 \times 10^{-5} \text{ g cm}^{-3}$ ; whereas, the decrease in temperature alone across the same depth interval yields an increase in density ( $\Delta\rho_{0,t,0}$ ) of  $9.1 \times 10^{-5} \text{ g cm}^{-3}$ . The larger change in

$\Delta\rho_{s,t,0}$  compared to  $\Delta\rho_{0,t,0}$  indicates that dissolved ions also contribute to the water column stability in the lake even though  $\rho_{s,t,0}$  is a conservative estimate due to the conservative nature of the conductance to salinity calculation.

Density calculations, based on conductivity data alone, lack contributions by uncharged species. Other constituents, such as dissolved silica, may play an important role in the density structure of the water column (e.g., McManus *et al.* 1992). Silicic acid is almost (95%) completely protonated, thus uncharged in freshwater systems with a pH similar to that in Lake Malawi (7.3–8.1; Gonfiantini *et al.* 1979). Dissolved silica concentrations in Lake Malawi range from approximately  $20 \mu\text{M}$  within the upper 100 m of the water column to  $170 \mu\text{M}$  at depths lower than 270 m (Eccles 1974; Johnson and Hecky personal communication 1992). Dissolved silica augments the increase in salinity, thus density, across the chemocline. The re-calculated increase in density ( $\Delta\rho_{s,t,0}$ ) is  $10.3 \times 10^{-5} \text{ g cm}^{-3}$  across the depth interval used above taking into account the dissolved silica, conductance, and temperature changes. The conservative calculations suggest that both temperature and dissolved constituents influence, on the same order of magnitude, the water-column stability in Lake Malawi during January (austral summer).

Several lines of evidence indicate that mixing across the chemocline occurs, but slowly or infrequently enough to maintain anoxic conditions in the monimolimnion. First, if the present salinity structure is maintained during austral winter then surface water temperatures cooler than  $22.6^\circ\text{C}$  would create an unstable water column. Water temperatures cooler than  $22.6^\circ\text{C}$  have been occasionally reported for the lake's surface, especially at the southern end of the lake. Second, a small rise in bottom-water temperature over time was previously reported for Lake Malawi. Eccles (1974) reported that bottom temperatures rose from  $22.1^\circ\text{C}$  in 1939 to  $22.56^\circ\text{C}$  in 1963; and Gonfiantini *et al.* (1979) reported bottom temperatures between  $22.66$  and  $22.76^\circ\text{C}$  below 500 m in 1976 at the same, deep-basin hydrograph station. The rise over time is attributed to heating from average geothermal inputs from the interior of the earth. Water temperatures at the deep-basin site from this study (ML4) are no warmer than  $22.70^\circ\text{C}$  below 300 m. The expanded temperature time series indicates that bottom-water temperatures do not increase uniformly over time. Presumably, cooler surface or near surface water is introduced to offset the previously proposed geothermal warming of the

monimolimnion. Finally, significant amounts of "bomb" produced tritium in the monimolimnion of Lake Malawi indicates that mixolimnion waters have exchanged with monimolimnion waters in the recent past (Gonfiantini *et al.* 1979).

A number of potential physical processes may allow mixing of surface or near surface waters with deeper portions of the water column. Density currents initiated by extraordinary evaporitic cooling of the surface waters at the southern arm of the lake during austral winter may extend into the monimolimnion (Eccles 1974, Beadle 1981). Exceptional cooling of nearshore surface water at other margins of the basin may promote localized insta-

bilities in the water column (Coulter and Spiegel 1991). Finally, turbidity channels and related structures, even in the deepest basin of the lake (Johnson and Ng'ang'a 1990), suggest that turbidity currents transport surface to near surface water to the lake floor. A temperature-salinity (T-S) plot at the deep-basin site provides evidence that multiple processes may be involved (Fig. 4). The T-S plot reveals two major semi-straight segments that represent above and below the thermocline. The lower portion of the curve can be divided into a number of shorter straight-line segments that correspond to various depth intervals within the mixolimnion and the monimolimnion (salinities  $> 127 \text{ mg kg}^{-1}$ ). The seg-

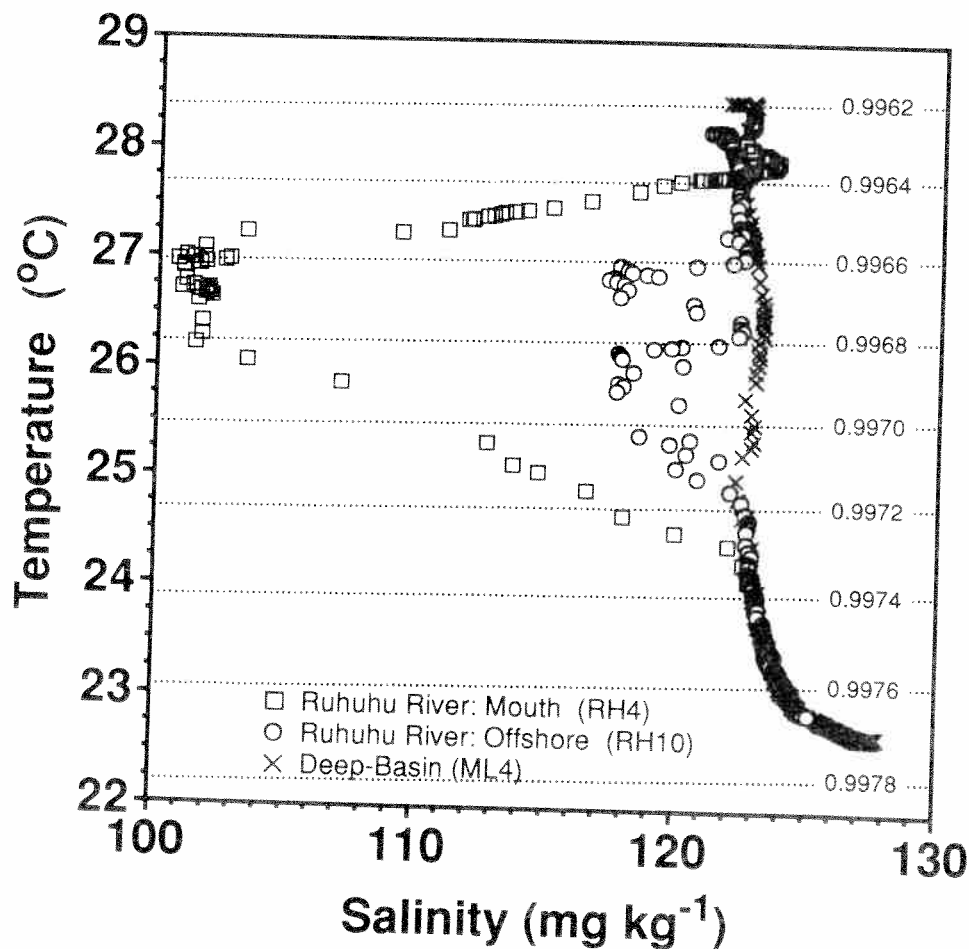


FIG. 4. Temperature-Salinity plots of CTD data collected at the Deep-Basin site ( $\times$ , ML4) and two stations offshore of the Ruhuhu River ( $\square$  RH4,  $\circ$  RH10). Salinities were calculated from conductivity, temperature, and pressure data using the equation of Hill *et al.* (1986). Isopycnals ( $\blacksquare$ ), relative to the lake's surface ( $\rho_{s,t,0}$ ), were calculated using the PVT equations of Chen and Millero (1977, 1986).



mentation suggests that surface or near surface water mixes more frequently with various depths within the mixolimnion than the mixolimnion mixes with the monimolimnion (Fig. 4). The orientation of the line segment in the monimolimnion is nearly parallel to calculated isopycnals and suggests that, once the barrier to deep-water mixing at the chemocline is breached, the water parcel can descend to the lake floor.

CTD profiles offshore of the Ruhuhu River highlight another mixing process in the basin (Fig. 3). The occurrence and spatial distribution of the mid-depth layer of low salinity suggests that the dispersal of fluvial inputs from the Ruhuhu is by an interflow pathway (Giovanoli 1990, Halfman and Scholz 1993). The hypothesis is supported by additional observations. River water is less saline than lake water. The Ruhuhu basin experienced monsoon-like rainfall for 2 days prior to profiling the delta. The relatively high oxygen concentrations in the mid-depth layer at the RH4 station is consistent with injection of water from an external source rather than typical open-lake processes. Finally, the layer coexists with a plume of turbid water that decreases in turbidity from the mouth of the river to farther offshore (Halfman and Scholz 1993). Mixing of the interflow layer with the rest of the lake apparently occurs at all the boundaries, i.e., T-S plots of two Ruhuhu stations (RH4 and RH10) reveal linear deviations from the least saline water to open-lake conditions above, below, and in front of the mid-depth layer (Fig. 4).

Recent seismic surveys of Ruhuhu Delta reveal that the shelf-break is incised by a number of deep (about 80 m), V-shaped, sublacustrine valleys (Scholz *et al.* 1993). The authors reasoned that the sharp change in gradient due to the juxtaposition of the Ruhuhu River with the border fault margin of the lake probably promotes erosion of the deep valleys especially during former low stands of the lake. Similar deeply incised, sublacustrine valleys are observed at the S. Rukuru Delta, another border-fault system, but are not observed at the deltas along shoaling margins in the survey. The geomorphology probably facilitates the injection of relatively fresh but turbid water at depth in the lake. Density calculations suggest that fluvial inputs during the rainy, warm season are probably restricted to depths above the thermocline because water temperatures of the river plume must cool below 23.6°C, water turbidities must significantly increase above the estimated concentrations, or a combination of the two to sink below the thermocline. However during exceptionally cold winters, water temperatures of the river may cool below

23.6°C which opens speculation that fluvial inputs are occasionally dense enough based on water temperature alone to promote vertical mixing throughout the mixolimnion and possibly into the monimolimnion. Temperature data from the Ruhuhu River are not available to confirm this speculation.

Interflow injection of fluvial material may exist at border-fault catchments that enter Lake Tanganyika. However, density currents and surface dispersal are associated with the two largest rivers in the lake: the Rusizi and Malagarazi rivers, respectively (Tiercelin and Mondeguer 1991). The discharge of the Omo River, which dominates the hydrology of Lake Turkana, is along the lake's surface (Halfman unpublished data). The variability highlights the complexities involved in developing an unifying model for the sedimentology or physical limnology of tropical rift lakes with the available data.

In summary, profiles of temperature and dissolved oxygen concentrations are consistent with previous reports, except for the inverse temperature gradient below 350 m. Specific conductance ( $\kappa_{25}$ ) of the water column typically increases with depth with approximately 50% of the increase between 160 and 240 m. The density gradient controls the extent of vertical mixing across the chemocline. Salinity augments temperature in defining the density structure across the chemocline during the rainy, warm season and may be the only barrier to vertical mixing across the chemocline during the windy, cool season. However, the historical trend in bottom-water temperatures, and other supporting evidence, suggests that the chemocline is not a permanent barrier to vertical mixing. Conductivity profiles offshore of the Ruhuhu River show a relatively fresh-water layer that is interpreted as an interflow injection of river discharge. Interflow injection introduces another mechanism to mix the water column of Lake Malawi.

#### ACKNOWLEDGMENTS

Many thanks are extended to Thomas C. Johnson, Christopher A. Scholz, Jim McGill, and the captain and crew of the *M/V Timba*, operated by the Malawi Department of Surveys, for their assistance in the field; and, to the governments of Malawi and Tanzania for research permission. Financial support was provided by Project SEPRO, Duke University Marine Laboratory, and by Jesse H. Jones Faculty Research Program and Department of Civil Engineering and Geological Sciences at the University of Notre Dame. Thanks are also extended to two reviewers of an earlier version of the manuscript.

## REFERENCES

- Beadle, L. C. 1981. *The inland waters of tropical Africa*. 2nd ed. New York, NY: Longman.
- Beauchamp, R. S. A. 1953. Hydrological data from Lake Nyasa. *J. Ecol.* 41:226-239.
- Chen, C. T., and Millero, F. J. 1977. The use and misuse of pure water PVT properties for lake waters. *Nature* 226:707-708.
- \_\_\_\_\_, and Millero, F. J. 1986. Precise thermodynamic properties for natural waters covering only the limnological range. *Limnol. Oceanogr.* 31:657-662.
- Coulter, G. W., and Spigel, R. H. 1991. Hydrodynamics. In *Lake Tanganyika and its Life*. ed. G.W. Coulter, pp. 49-75. New York, NY: Oxford University Press.
- Crossley, R. 1984. Controls on sedimentation in Malawi rift valley, central Africa. *Sedimentary Geol.* 40:33-50.
- Eccles, D. H. 1962. An internal wave in Lake Nyasa and its probable significance in the nutrient cycle. *Nature* 194:832-833.
- \_\_\_\_\_. 1974. An outline of the physical limnology of Lake Malawi (Lake Nyasa). *Limnol. Oceanogr.* 19:730-742.
- Ferro, W. 1977. *A limnological baseline survey of the Chintechi area of Lake Malawi*. FAO, Rome.
- Finney, B. P., and Johnson, T. C. 1991. Sedimentation in Lake Malawi (east Africa) during the past 10,000 years: a continuous paleoclimatic record from the southern tropics. *Palaeogeogr., Palaeoclimat., Palaeoecol.* 85:351-366.
- Giovanoli, F. 1990. Horizontal transport and sedimentation by interflows and turbidity currents in Lake Geneva. In *Large Lakes*, eds. M. Tilzer and C. Seruya, pp. 175-195. New York, NY: Springer-Verlag.
- Gonfiantini, R., Zuppi, G. M., Eccles, D. H., and Ferro, W. 1979. Isotope investigations of Lake Malawi. In *Isotopes in Lake Studies*. International Atomic Energy Agency Panel Proceeding Series STI/PUB/511.
- Halfman, J. D., and Scholz, C. A. 1993. Suspended sediments in Lake Malawi, Africa: A reconnaissance study. *J. Great Lakes Res.* 19:499-511.
- Hill, K. D., Dauphinee, T. M., and Woods, D. J. 1986. The extension of the practical salinity scale 1978 to low salinities. *IEEE J. Ocean. Engr.* OE-11:109-112.
- Jackson, P. B. N., Iles, T. D., Harding, D., and Fryer, G. 1963. *Report on a survey of northern Lake Nyasa by the Joint Fisheries Research Organization 1953-1955*. Gov. Printer, Zomba.
- Johnson, T. C., and Ng'ang'a, P. 1990. Reflections on a rift lake. In *Lacustrine basin exploration—case studies and modern analogs*, ed. B.J. Katz, pp. 113-135. Tulsa, OK: AAPG Memoir #50.
- \_\_\_\_\_, Davis, T. W., Halfman, B. M., and Vaughan, N. D. 1988. *Sediment core descriptions: Malawi '86: Lake Malawi, East Africa*. Duke Univ. Mar. Lab. Project PROBE Tech. Rep.
- McManus, J., Collier, R. W., Chen, C. T., and Dymond, J. 1992. Physical properties of Crater Lake, Oregon: A method for the determination of a conductivity- and temperature-dependent expression for salinity. *Limnol. Oceanogr.* 37:41-53.
- Owen, R. B., Crossley, R., Johnson, T. C., Tweddle, D., Kornfield, I., Davison, S., Eccles, D. H., and Engstrom, D. E. 1990. Major low levels of Lake Malawi and implications for speciation rates in cichlid fishes. In *Proceedings of the Roy. Soc. of London* 240:519.
- Pike, J.G. 1964. The hydrology of Lake Nyasa. *J. Instit. Water Engr.* 18:542-564.
- Scholz, C. A., and Rosendahl, B. R. 1988. Low lake stands in Lakes Malawi and Tanganyika, East Africa, delineated with multi-fold seismic data. *Science* 240:1645-1648.
- \_\_\_\_\_, Johnson, T. C., and McGill, J. W. 1993. Deltaic sedimentation in a rift valley lake: New seismic reflection data from Lake Malawi (Nyasa), East Africa. *Geology* 21:395-398.
- Tiercelin, J.-J., and Mondeguer, A. 1991. The geology of the Tanganyika Trough. In *Lake Tanganyika and its Life*. ed. G.W. Coulter, pp. 7-48. New York, NY: Oxford University Press.

Submitted: 1 February 1993

Accepted: 7 June 1993